Journal of Applied Polymer Science

Development of Antimicrobial Stainless Steel via Surface Modification with N-Halamines: Characterization of Surface Chemistry and N-Halamine Chlorination

Luis J. Bastarrachea, Julie M. Goddard
Department of Food Science, University of Massachusetts, Amherst, Massachusetts 01003
Correspondence to: J. M. Goddard (E-mail: goddard@foodsci.umass.edu)

ABSTRACT: N-halamine modification of materials enables the development of antimicrobial materials whose activity can be regenerated after exposure to halogenated sanitizers. Surface and bulk modification of polymers by N-halamines has shown great success, however, modification of inorganic substrates (e.g., stainless steel) remains an area of research need. Herein, we report the covalent surface modification of stainless steel to possess rechargeably antimicrobial N-halamine moieties. Multilayers of branched polyethyleneimine and poly(acrylic acid) were immobilized onto the surface of stainless steel and the number of N-halamines available to complex chlorine was quantified. Samples were characterized through contact angle, Fourier transform infrared spectroscopy, ellipsometry, dye assay for amine quantification, and X-ray photoelectron spectroscopy. Increasing the number of multilayers from one to six increased the number of N-halamines available to complex chlorine from 0.30 ± 0.5 to 36.81 ± 5.0 nmol cm^{-2}. XPS and FTIR confirmed successful covalent layer-by-layer deposition of the N-halamine multilayers. The reported layer-by-layer deposition technique resulted in a greater than seven-fold increase of available N-halamine compared to prior reports of N-halamine surface modifications. The N-halamine modified steel demonstrated antimicrobial activity (99.7% reduction) against the pathogen *Listeria monocytogenes*. Such surface modified stainless steel with increased N-halamine functionality, and therefore potential for rechargeable antimicrobial activity, supports efforts to reduce cross-contamination by pathogenic organisms in the food and biomedical industries. © 2012 Wiley Periodicals, Inc. J. Appl. Polym. Sci. 000: 000–000, 2012

KEYWORDS: biological applications of polymers; ESCA/XPS; FT-IR; surface modification; nanolayers

Received 21 December 2011; accepted 27 March 2012; published online
DOI: 10.1002/app.37806

INTRODUCTION

Cross-contamination of pathogenic microorganisms is a major concern in the food and biomedical industries because of the impact to public health as well as the resulting financial impact of medical expenses.[1,2] In the food industry, the growth and cross-contamination of pathogens like *Listeria monocytogenes*, *Escherichia coli*, and *Salmonella* spp. on the surface of food contact materials (work tables, conveyor belts, processing equipment) as well as noncontact materials (ventilation ducts, door knobs, etc.) pose a public health risk. There is also a substantial potential for economic losses due to the proliferation of spoilage microorganisms and resulting product loss. Further, some microorganisms are able to form stable communities called biofilms, which increases their resistance to traditional cleaning and sanitization methods.[3–5]

Stainless steel is a commonly used material in food processing facilities as well as in fabrication of biomedical devices.[5–7] However, several studies have shown its ability to harbor biofilms composed of microorganisms from different genera, including *Listeria*, *Staphylococcus*, *Escherichia*, *Bacillus*, and *Pseudomona*.[8–13] Currently, there is no available strategy to totally prevent or control the formation of biofilms. The most common techniques used are the application of disinfectants and heat, which are less effective on microorganisms that have formed a stable biofilm.[3] There is therefore a continued need to reduce the adhesion, survival, and cross-contamination of pathogenic and spoilage organisms on stainless steel. Development of antimicrobial materials for which the antimicrobial activity is long-lasting and does not diminish via migration of the antimicrobial agent can help to support current cleaning and sanitization protocols in improving food safety.

N-halamines are antimicrobial structures in which a stable nitrogen-halogen complex can be rechargeably formed after contact with halogenated sanitizers (e.g., sodium hypochlorite,

bromophors/iodophors). N-halamines can exist as amines, amides, or imides and the halogen position can be occupied by an atom of chlorine, bromide, and iodide. N-halamines composed by amines exhibit higher stability than those composed by amides, which in turn are more stable than those composed by imides.[14] The stability is given by the ability of the N-halamine to provide an electron to the halogen atom, working as a sort of resonance system and avoiding the separation of the halogen from the rest of the molecule due to the loss of one of its electrons. Probably the most important feature of N-halamines is their ability to be regenerated with solutions containing the corresponding halogen, which makes them able to provide antimicrobial activity repeatedly. The halogen is released once it gets in contact with microorganisms, inactivates them, and the N-halamines can be regenerated again (with sodium hypochlorite/bleach commonly), making them ready for another cycle of disinfection.[14] N-halamine functionalized materials have been developed for a range of applications such as biocides in swimming pools and spas, disinfectants in water filtration systems, disinfectants of recreation water, and so on.[15] They have also been incorporated in fabrics to be used in the production of different types of clothes.[4–16] Both soluble and insoluble N-halamines have been developed with demonstrated activity against microorganisms, and both bulk and surface modification techniques have been employed to impart N-halamine activity to materials.[14,16–19] Surface modification in which the N-halamine moiety is *covalently* attached to a materials surface decreases the likelihood of N-halamine migration from the substrate, a potential regulatory benefit.[15,20] A few reports have been published on surface modification of polymeric materials with N-halamines; however, there are no reports of such modifications on inorganic substrates like stainless steel.

The overall goal of this work was to modify the surface of 316 stainless steel to possess rechargeably antimicrobial N-halamine functionality, and to increase the number of N-halamines by a sequential layer-by-layer deposition process. The objectives were to modify the surface of stainless steel through the layer-by-layer deposition of increasing number of layers of covalently linked branched polyethyleneimine (PEI) and polyacrylic acid (PAA), to evaluate the capacity to retain and release chlorine, and finally to characterize the materials through surface analytical techniques to confirm the chemical modification. The number of N-halamines and primary amines increased with the number of multilayers immobilized. Covalent bond formation between the applied polymers and stainless steel was confirmed through FTIR, ellipsometry, and XPS. No significant difference between control samples and treated samples was observed in contact angle ($P > 0.05$).

EXPERIMENTAL PROCEDURE

Materials

Stainless steel 316L #2B and #8 finish (non-mirror and mirror-polished, respectively) was purchased from McMasterr-Carr (Chicago, IL). Isopropanol, acetone, sulfuric acid, hydrogen peroxide, toluene, hydrochloric acid (12 N), sodium hydroxide and HPLC grade water, and sodium chloride were purchased from Fisher Scientific (Pittsburgh, PA). The silane-coupling agent 3-glycidoxypropyltrimethoxysilane (GOPTS), sodium hypochlorite (5% chlorine), and AO7 dye [Orange (II) (Cert)] were purchased from Acros Organics (Fair Lawn, NJ). Branched PEI was purchased from Sigma-Aldrich (St. Louis, MO), and poly (acrylic acid) (PAA) was purchased from Scientific Polymer Products (Ontario, NY). N-hydrosuccinimide (NHS) was purchased from Acros Organics. 1-(3-Dimethylaminopropyl)-3-ethylcarbodiimide hydrochloride (EDC-HCl) was purchased from ProteoChem (Denver, CO). DPD total chlorine reagent powder was from Hach Company (Loveland, CO). *Listeria monocytogenes* FSL-J1-225 Scott A was graciously provided by the laboratory of Dr. Lynne McLandsborough. Tryptic soy broth (TSB), tryptic soy agar (TSA), and neutralizing buffer (NB) were purchased from Becton, Dickinson and Company (Sparks, MD).

Stainless Steel Surface Modification

Two finishes of 316L stainless steel were used in this work. Because of its widespread application in commercial food processing, a 2B finish was used for most of the work. However, the inherent roughness of 2B finished steel introduces complications when using analytical techniques which require very smooth substrates to obtain meaningful quantitative data. For these reasons, a #8 finish (mirror-polished steel) was used to prepare samples for FTIR, ellipsometry, and AFM analysis, while 2B finished steel was used for samples subjected to XPS, dye assay, contact angle, and antimicrobial activity assays. Regardless of finish, samples were cleaned and modified in the same manner. Stainless steel samples were cut into 1 × 2.5 cm coupons. Before surface modification, samples were subjected to cleaning, first with isopropanol then with acetone, and finally with deionized (DI) water under sonication (two 10 min cycles per solvent). Samples were then dried with purified air and immersed in piranha solution, prepared by mixing carefully sulfuric acid and hydrogen peroxide in a 7 : 3 volumetric ratio of sulfuric acid and 30% hydrogen peroxide for 20 min to clean the surface of the samples and create hydroxyl groups. After piranha solution treatment, samples were rinsed with DI water, dried with purified air, and left shaking overnight in toluene to precondition the surface before solvent-based silanization. Samples which had undergone piranha treatment and toluene soaking were dried with purified air and stored in clean glass Petri dishes as control samples. Samples that were going to be subjected to further chemical modification were then immersed in a solution of toluene containing 2% (v/v) of the silane-coupling agent GOPTS and shaken for 10 min. Once treated with GOPTS, samples were rinsed with copious toluene, dried with purified air, and heated for 2 h at 80°C to promote covalent bond formation between the oxidized stainless steel surface and GOPTS. Cured, GOPTS-treated samples were stored in clean glass Petri dishes as "GOPTS" treatment. The rest of the samples were treated as follows: to apply a single multilayer of PEI and PAA, samples were first immersed in a 0.1*M* phosphate buffer solution, pH 7.8, containing 5 mg mL^{-1} of branched PEI, and the zero-length cross-linker EDC–HCl and NHS in a concentration of 50 and 5 m*M* (respectively), and shaken for 30 min. Then, after having been rinsed in copious DI water and dried with purified air, samples were immersed in a 0.1*M* phosphate buffer solution, pH 7.8, containing 5 mg mL^{-1} of PAA and the same

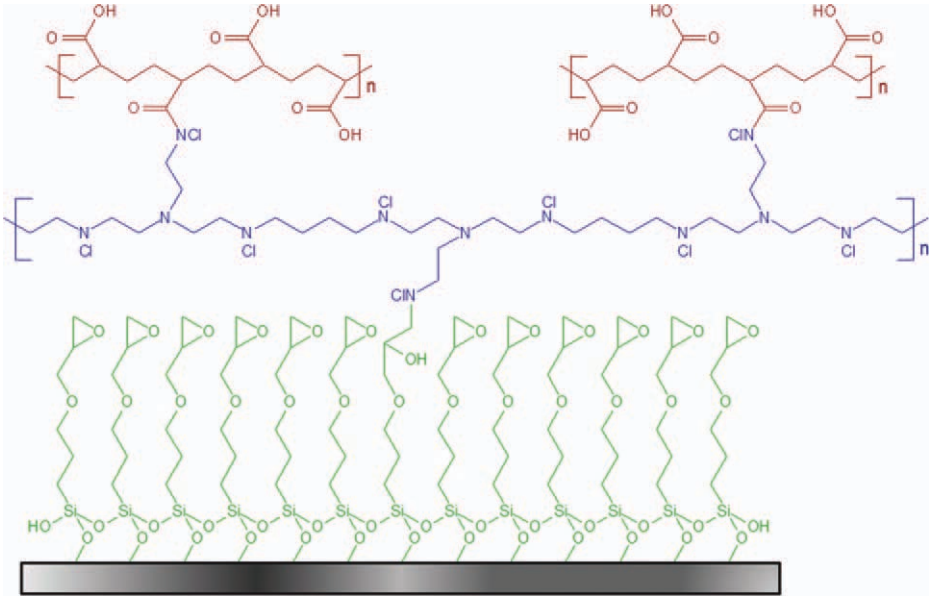

Figure 1. Schematic of chlorinated, N-halamine-modified stainless steel prepared by layer-by-layer deposition technique. [Color figure can be viewed in the online issue, which is available at wileyonlinelibrary.com.]

concentrations of EDC–HCl and NHS, shaken for 30 min, rinsed in copious DI water, and dried with purified air. The described procedure was repeated until completing up to six multilayers. Samples were randomly selected after each multilayer deposition to be subjected to surface analysis as described below. Figure 1 illustrates the overall chemistry of the chlorinated N-halamine surface modified stainless steel.

N-Halamine Activation and Determination of Chlorination

Samples from the different treatments prepared as explained earlier were shaken for 15 min in individual test tubes containing DI water with 3000 ppm of chlorine, prepared by making the corresponding dilution from a sodium hypochlorite solution containing 5% of free chlorine. The chlorine content of the sodium hypochlorite solution was confirmed previously through the standard method D 2022–89, in which the available chlorine content is determined through an iodometric titration with $Na_2S_2O_3$ 0.1*N*.[21] Samples were rinsed with copious DI water after the 15 min of shaking, and dried with purified air. Then, the samples were transferred to individual test tubes with DI water. The ability of N-halamines to complex chlorine was determined through a modified N,N-diethyl-p-phenylenediamine (DPD) assay. DPD reagent was prepared by mixing one packet of DPD total chlorine reagent powder with 1 mL of DI water. A volume of 50 μL of DPD reagent was applied per every mL of DI water contained in the individual test tubes. Then, the samples were shaken for 2 min and the absorbance of the solutions in contact with them was measured at 512 nm. The chlorine concentration of the solutions was determined from a standard curve of sodium hypochlorite in DI water. The chlorination of N-halamines in nmol cm^{-2} was calculated by taking into account the volume of DI water in contact with the samples and the samples' dimensions. This procedure was performed three times (three replicates), with four samples per treatment in every replicate.

Contact Angle

Advancing (θ_A) and receding (θ_R) water contact angles were determined with a DSA100 (Kruss, Hamburg, Germany). A volume of 2.5 μL HPLC grade water was applied at a rate of 15 μL min^{-1} with automatic dispenser. Measurements were performed under atmospheric conditions and were analyzed using the Drop Shape Analysis software, version 1.91.0.2 (Kruss, Hamburg, Germany). Hysteresis (H) was obtained from the difference between θ_A and θ_R. A total of three replicates were performed for this evaluation, with three samples per treatment in every replicate and three measurements were done in every sample (nine measurements per replicate).

Fourier Transform Infrared (FTIR) Spectroscopy

Mirror-polished stainless steel (316, 0.036″ thick) was used as a substrate for multilayer deposition for FTIR, ellipsometry, and AFM measurements (described below), to avoid artifacts resulting from inherent roughness in #2B finished stainless steel. Changes in surface chemistry were determined with an IRPrestige 21 spectrometer (Shimadzu Corp., Tokyo, Japan). Absorbance was measured in three different spots of each of three samples per treatment with a Monolayer Grazing Angle Accessory (Specac, Orpington Kent, UK) at an angle of incidence of 60°. A resolution of 4 cm^{-1} and a total of 200 scans were applied for every spot using square triangle apodization. Control samples (i.e., piranha cleaned steel) were used as the background. The spectra were collected with IRsolution software (Shimadzu, Tokyo, Japan), and after baseline correction, atmospheric correction and smoothing (20 points), spectra were analyzed with the Knowitall software (Biorad Laboratories, Philadelphia, PA). The areas of representative peaks were calculated with the IRsolution software. A total of three replicates were performed, with three samples per treatment in every replicate.

Ellipsometry

Before determination of thicknesses by ellipsometry, the refractive indices of PEI, PAA, and GOPTS were confirmed with a

digital refractometer from Sper Scientific model 300034 (Sper Scientific, Scottsdale, AZ). The thicknesses of the increasing multilayers of the different treatments were determined with a Rudolph research model auto SL-II automatic ellipsometer (Rudolph Research Analytical, Hackettstown, NJ) with an angle of incidence of 70° from the normal. The light source was a He–Ne laser with $\lambda = 632.8$ nm. Measurements were done in three different spots of a single sample. Three replicates were done for this evaluation, with three samples per treatment in every replicate.

Atomic Force Microscopy

Mirror-polished stainless steel samples were cleaned and modified as described above for analysis of nanoscale surface topography by atomic force microscopy (AFM). AFM was used to characterize the roughness and surface morphology of the control and modified stainless steel samples using a Dimension 3100 Atomic Force Microscope (Digital Instruments, Santa Barbara, CA). Tapping mode tips (Veeco, phosphorus n-doped Si, f_0: 312–342 kHz) were used on cantilevers having a resonance frequency in the range of 290–410 kHz. AFM images were flattened, filtered, and analyzed through the SPIP software (Scanning Probe Image Processor, Image Metrology, Denmark).

Acid Orange 7 (AO7) Dye Assay

The quantification of primary amines on the samples' surface was performed as follows. Samples were immersed in individual test tubes containing 1 m*M* of AO7 dye [Orange (II) (Cert), Acros Organics, Fair Lawn, NJ] in DI water adjusted to a pH of 3 by hydrochloric acid. After the 3 h of shaking, the samples were rinsed in copious DI water (pH = 3) to remove noncomplexed dye. Samples were then transferred to individual test tubes containing DI water adjusted to a pH of 12 by sodium hydroxide to desorb the absorbed dye. Samples were then shaken for 15 min and the absorbance of the solutions in contact with the samples was measured at 455 nm. The AO7 concentration was determined from a standard curve of AO7 in DI water (pH = 12) and the primary amines content on the surface of the samples was calculated based on such concentration and the samples' dimensions.[22] Three replicates were performed for this assay, with three samples per treatment in every replicate.

X-Ray Photoelectron Spectroscopy

XPS analysis was performed with a Physical Electronics Quantum 2000 (Physical Electronics, Chanhassen, MN) with Al Kα excitation at a spot size of 100 μm at 25 W. Spectra were obtained at an angle of 45° relative to the samples' plane. Survey scans of every sample were collected at a pass energy of 187.85 eV with a step size of 1.6 eV. High resolution spectra were collected at a pass energy of 46.95 eV and with a step size of 0.4 eV. Atomic concentrations and high resolution spectra were analyzed with the MultiPak software version 6.1A (Physical Electronics, Chanhassen, MN). After linear background subtraction, high resolution spectra were fitted with the Gaussian-Lorentzian model (90% Gaussian was applied).

Antimicrobial Activity Assay

Unmodified and stainless steel modified with six N-halamine multilayers were subjected to an antimicrobial activity assay. *Listeria monocytogenes* was used as a model organism to demonstrate antimicrobial activity because of its importance in food safety, having been reported to be the pathogen responsible for the most food-borne illness related deaths.[23] Overnight cultures were grown in TSB and diluted with water to a final concentration of approximately 10^5 CFU mL^{-1}. Stainless steel coupons (1 × 2.5 cm^2) were submerged in 4 mL of an aqueous suspension of *Listeria monocytogenes* and incubated with rotation at 32°C. After 6 h, suspensions were enumerated by serial dilution in saline water (0.9% NaCl) followed by plating on TSA agar and incubation for 48 h at 37°C. Colonies were counted and antimicrobial activity was recorded as the log reduction in CFU mL^{-1}.

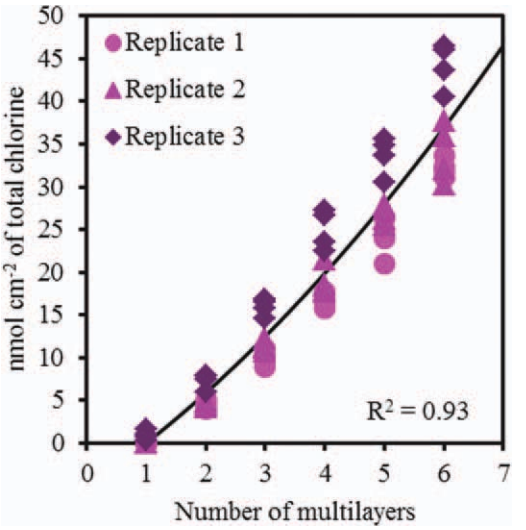

Figure 2. Relationship observed between the N-halamine chlorination and the number of covalently bound multilayers. [Color figure can be viewed in the online issue, which is available at wileyonlinelibrary.com.]

Statistical Analysis

One-way analysis of variance (ANOVA) followed by Tukey's pairwise comparisons was conducted between treatments using Minitab version 16.1.1 (Minitab, State College, PA) with a confidence interval of 95%. As appropriate, regression analysis was also evaluated at a 95% confidence interval.

RESULTS AND DISCUSSION

N-Halamine Activation and Determination of Chlorination

The ability of control and multilayer N-halamine modified stainless steel to complex with chlorine after contact with 3000 ppm sodium hypochlorite was quantified by a modified DPD assay (Figure 2). No chlorination was observed for the GOPTS treated stainless steel, as expected. The Control (clean stainless steel) treatment exhibited trace chlorination, likely due to hydrophilic behavior brought by the piranha solution, however, this trace chlorination was not significantly different from GOPTS treated ($P > 0.05$). The level of N-halamine chlorination increased with increasing multilayer deposition, with a quadratic relationship from one to six multilayers ($P > 0.05$).

Contact Angle

Water contact angles (advancing, receding, and hysteresis) were measured for control and modified steel to determine the effect

Table I. Advancing and Receding Water Contact Angle, and Contact Angle Hysteresis

Treatment	Advancing contact angle θ_A (Degrees)	Receding contact angle θ_R (degrees)	Contact angle hysteresis H (degrees)
Control	37.11 ± 4.5^{ac*}	33.79 ± 4.0^{a}	3.32 ± 0.7^{a}
GOPTS	64.97 ± 3.0^{b}	55.07 ± 7.3^{b}	9.90 ± 4.4^{b}
One multilayer	41.01 ± 3.6^{a}	34.30 ± 3.4^{a}	6.71 ± 1.2^{ab}
Two multilayers	27.37 ± 6.8^{ac}	23.74 ± 5.9^{a}	3.63 ± 1.7^{a}
Three multilayers	23.60 ± 4.9^{c}	19.96 ± 5.0^{a}	3.63 ± 0.8^{a}
Four multilayers	27.84 ± 0.9^{ac}	23.40 ± 0.6^{a}	4.45 ± 1.1^{a}
Five multilayers	32.45 ± 12.1^{ac}	27.20 ± 10.6^{a}	4.45 ± 1.5^{ab}
Six multilayers	28.64 ± 3.9^{ac}	23.65 ± 4.4^{a}	4.99 ± 0.6^{ab}

*Values are means of three replicates ± 1 SD. Treatments with the same letter within the same column are not significantly different ($P > 0.05$).

of N-halamine multilayer deposition on wettability (Table I). The only treatment that exhibited significantly different advancing contact angle (θ_A) ($P < 0.05$), when compared with the rest of the treatments was GOPTS treated. Such behavior can be attributed to the hydrophobic nature of GOPTS, which made the stainless steel surface have a higher value of θ_A compared with the rest of the treatments. None of the treatments of steel modified with N-halamine forming multilayers (one to six multilayers) was significantly different from the Control in θ_A. However, the values of θ_A for one multilayer and three multilayers were significantly different ($P < 0.05$), suggesting an increase in hydrophilicity as the number of multilayers increases from one to three. It is likely that the hydrophobic influence of the underlying GOPTS monolayer is more evident with only a single multilayer than when several multilayers are immobilized. None of the treatments of steel modified with N-halamine forming multilayers was significantly different from the Control in θ_R ($P > 0.05$). As observed with θ_A, and the only treatment significantly different from the rest was that of GOPTS treated steel ($P < 0.05$). A substantial variability was observed from the multilayer modified steel in the measured values of θ_A and θ_R. The more heterogeneous or rough a surface is, the more evident the fluctuations among contact angle measurements will be.[24] The reason behind this phenomenon may be related to a non-uniform distribution of the introduced chemical species on the substrate's surface (stainless steel in this case), creating zones of varying hydrophilic or hydrophobic nature.[25,26] Such lack of uniformity may also explain the observed variability in the values of H. Some areas in the sample may exhibit a higher tendency to absorb water, whereas other areas will tend to repel it. In addition, surface topography can also increase or decrease adsorption of water, which relates to the surface roughness. Hence, the effect in wettability caused by a change in surface chemistry can be amplified by an irregular surface, leading to a less predictable behavior in H.[27]

FTIR Spectroscopy

The results from grazing angle FTIR analysis confirmed that the surface of the treated stainless steel possessed increasing quantities of N-halamines with increasing multilayer deposition. Figure 3 shows representative spectra from 0 (GOPTS treated) to six multilayers in the range from 1875 to 1365 cm^{-1}, which includes absorbance bands characteristic of amine, amide, and carbonyl functionalities. A characteristic band was observed at around 1535 cm^{-1}, which can be attributed to the N—H bond in plane bend of secondary amides. An increasing absorbance in this band suggests the formation of covalent bonds between the primary amines of PEI and the carboxylic acid groups of PAA, an important observation which supports the covalent nature of the N-halamine modification of stainless steel. A more subtle band was observed at about 1638 cm^{-1}, which corresponds to the scissors vibration of primary amines. Another band formed at about 1680 cm^{-1}, which can be related to the C=O stretch of secondary amides. At about 1750 cm^{-1}, a band was exhibited which may suggest the formation of acid anhydrides. The chlorine from unreacted EDC–HCl may have favored the formation of acid anhydrides, which can form from the condensation of the polar heads of two carboxylic acids in the presence of chlorine. A less evident band was seen at 1420 cm^{-1}, belonging to the O—H bond in plane bend of carboxylic acids.[28] The area beneath the spectra in the range of 1680–1395 cm^{-1} was calculated for stainless steel modified with one to six multilayers (Figure 4). The area in the chosen range was observed to increase with a quadratic relationship ($P < 0.05$) as the number of multilayers increased. This observation is in good agreement

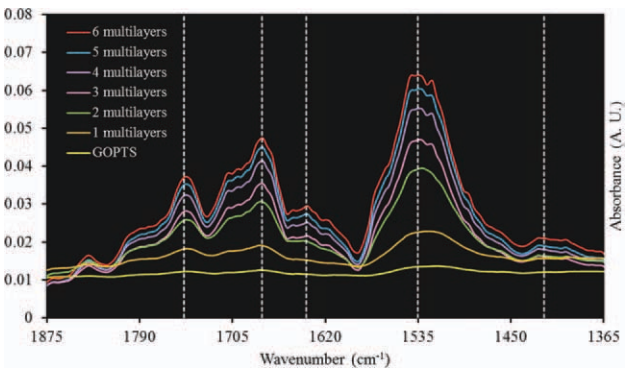

Figure 3. Representative FTIR spectra between 1875 and 1365 cm^{-1} of GOPTS treated steel (bottom) to steel modified with up to six N-halamine forming multilayers (top). [Color figure can be viewed in the online issue, which is available at wileyonlinelibrary.com.]

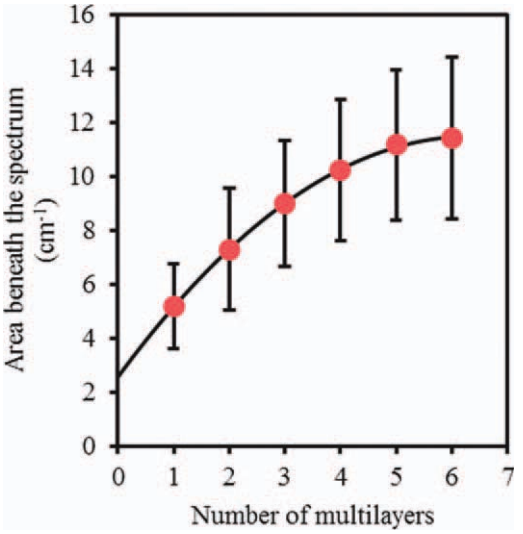

Figure 4. Relationship between the area beneath the spectra and the number of multilayers. [Color figure can be viewed in the online issue, which is available at wileyonlinelibrary.com.]

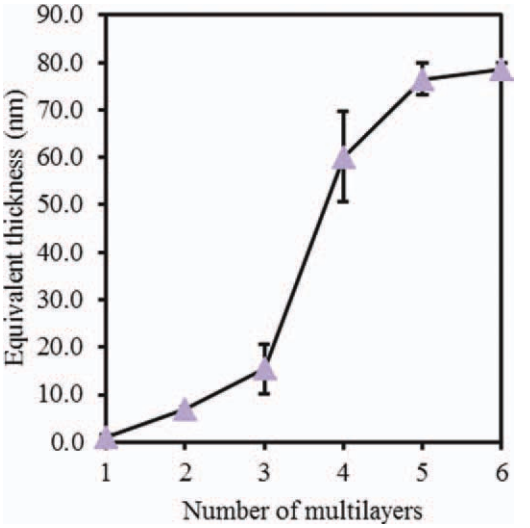

Figure 5. Thickness of N-halamine forming multilayers as determined by spectroscopic ellipsometry. Values are means of three replicates ± 1 standard deviation. [Color figure can be viewed in the online issue, which is available at wileyonlinelibrary.com.]

with prior FTIR analysis of PEI attached to steel, which show characteristic bands in the 1200–1600 cm^{-1} range.[29]

Ellipsometry

Spectroscopic ellipsometry was performed to quantify the equivalent thickness of increasing numbers of N-halamine forming multilayers after deposition onto stainless steel (Figure 5). A non-linear behavior was observed between the number of multilayers and the increasing thickness, in which a substantial increase in thickness took place from three to four multilayers. From four to six multilayers, there was a notably less pronounced increase in corresponding thickness with deposition of each sequential multilayer. Different phenomena can explain this condition. From one to three multilayers, a higher proportion of reactive groups from the PEI and/or PAA polymers may have bound with available surface groups on the stainless steel substrate, leaving fewer groups available for ionization and/or swelling which leads to a less pronounced increase in thickness. This would imply that the behavior shown by the increase in thickness as the number of multilayers increases depends not only on the amount of PEI or PAA deposited, but in the spatial arrangement in which such deposition takes place. At the pH of the phosphate buffer used (7.8), most of the carboxylic acids of PAA have a negative charge ($pK_a \approx 4.8$).[30] On the other hand, above a pH of 3, about 70% of the amine groups of PEI are protonated.[31] It can be assumed that as more available sites of interaction are formed (after having covered must of the substrate's surface), and more positively charges from PEI are exposed, more negatively charged PAA chains will diffuse and be attracted to the previously added PEI chains by electrostatic interactions, leading finally to the formation of covalent bonds. This phenomenon may be another reason behind the observed behavior in the increase of thickness. In addition, a non-linear growth in the thickness of polymer multilayers can be explained by the reorganization and interdiffusion of any of the polymers within multilayer system. Another possible phenomenon is the formation of "islands" from the application of the first layer or multilayer, instead of a uniform layer. Such islands can later join together (coalesce) as more layers of polymers are deposited. This has been observed in previous works involving layer-by-layer deposition of PEI and PAA, which suggests an increase in roughness from the formation of such islands with increasing number of deposited multi layers.[32,33] Our observations on multilayer thickness as determined by ellipsometry are also in good agreement with previously published work. Deposition of carbon nanofibers in four PEI/PAA bilayers on polyurethane foam resulted in a total thickness of 87 nm.[34]

A power relationship was found between area beneath spectra/thickness and number of multilayers (Figure 6). This behavior

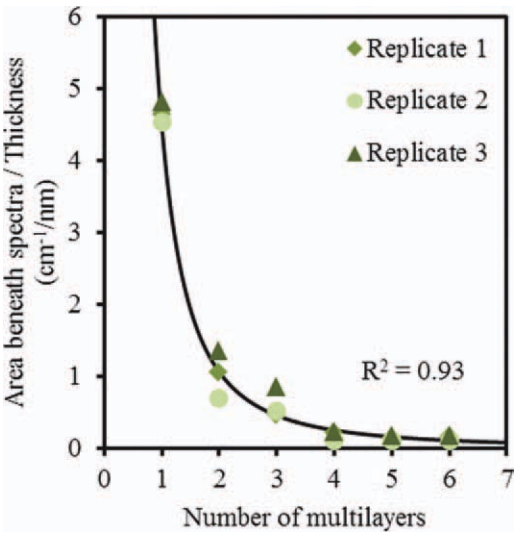

Figure 6. Relationship found between the ratio of the area beneath spectra/thickness and number of multilayers. [Color figure can be viewed in the online issue, which is available at wileyonlinelibrary.com.]

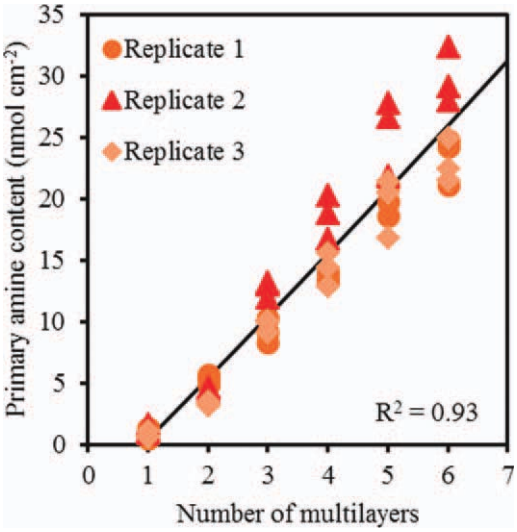

Figure 7. Relationship observed between the primary amine content and the number of covalently bound N-halamine forming multilayers from one to six multilayers. [Color figure can be viewed in the online issue, which is available at wileyonlinelibrary.com.]

may support the idea of the initial formation of "islands" in the surface of the substrate, which represent a low initial concentration of the chemical species attached. However, the average initial thickness is low if it is correlated with the initial concentration of the polymers. Such ratio decreases as the number of multilayers increases (at least in the analyzed range), as multilayer thickness increases in a non-linear behavior.

Acid Orange 7 (AO7) Dye Assay

An increase in the primary amine content was observed as the number of multilayers increased (Figure 7), proportional to the increase in N-halamine chlorination (Figure 2). N-halamines are capable of forming on amines (both primary and secondary), amides, and imides, with amines reported to stabilize the N-halamine: halogen complex most strongly.[14] Branched PEI has a ratio of primary, secondary and tertiary amines of 1 : 2 : 1. Our results suggest that approximately 50% of the available amines on the PEI component of each multilayer were able to complex chlorine as antimicrobial N-halamines.

X-ray Photoelectron Spectroscopy (XPS)

XPS survey scans as well as high resolution C 1s and Si 2p spectra were performed to quantify the change in surface atomic composition and specific bond formation after stainless steel was surface modified by GOPTS treatment and with each layer-by-layer multilayer deposition (Table II). The oxidation of stainless steel in the control samples as a result of piranha treatment was confirmed by the high oxygen percentage. GOPTS treatment introduced 3.48% Si, as expected from successful silanization. At an incidence angle of 45°, the applied beam has an analysis depth of approximately 2.5 nm, whereas the first multilayer of PEI and PAA was determined by ellipsometry to present a thickness of ~1.1 nm. As such, it is expected that the one multilayer atomic composition will contain a small amount of silicon and chromium, as observed, as the beam is interrogating the underlying GOPTS. From two to six multilayers, however, the overall thickness comprised of PEI/PAA exceeds the XPS sampling depth of 2.5 nm, and the resulting atomic compositions are expected to be similar for each increasing multilayer. Our experimentally determined atomic compositions support this hypothesis. The values obtained closely approximated the theoretical proportion of carbon, oxygen, and nitrogen present in a mixture of equal amounts of PEI and PAA (neglecting the presence of hydrogen, which is undetectable by XPS) and taking into account their monomeric formulas:

—$(C_2H_4NHC_2H_4N(C_2H_4NH_2)C_2H_4NH)_n$— for PEI and —$(CH_2CH(COOH))_n$— for PAA. Theoretical atomic percentages are calculated as follows: 52.5% C, 22% O, 16% N, and 9.5% H (58% C, 24.3% O, and 17.7% N taking only C, O, and N into account). The observed deviations from theoretical atomic compositions (higher carbon and oxygen percentages, and lower nitrogen percentage) are small, but such subtle deviations suggest that signal from the GOPTS is still detectable, which further supports the formation of non-uniform islands, as described above. Alternatively, it is possible that the ratio of PAA: PEI within each multilayer is not unity, but rather there may be enhanced deposition of PAA over PEI.

Figure 8 shows representative survey XPS spectra obtained from control, GOPTS treated, single multilayer, and two to six multilayer modified stainless steel. Table III displays the relative percentages of the chemical species found from the high resolution spectra of C 1s and Si 2p in the evaluated treatments. For the case of the control and GOPTS treatments, the deconvolution of the high resolution spectrum of C 1s exhibited the presence of the chemical species C—C/C—H, C—O, and C=O/O—C=O, in the binding energy ranges of 284–285 eV, 286–287 eV, and 287–288 eV, respectively [Figure 9(A,B)]. The deconvolution of

Table II. Representative Atomic Concentrations Obtained From XPS (%)

Treatment	C	N	O	Si	Cr	Mn	Co	S	Mo
Control	17.52		55.22		10.62	3.15	5.06	4.90	3.54
GOPTS	32.02		54.68	3.48	4.20		3.31		
One multilayer	54.62	8.66	32.23	1.75	2.74				
Two multilayers	67.47	11.41	21.12						
Three multilayers	67.81	13.70	18.49						
Four multilayers	67.36	12.57	20.07						
Five multilayers	65.71	13.7	20.59						
Six multilayers	66.72	12.87	20.4						

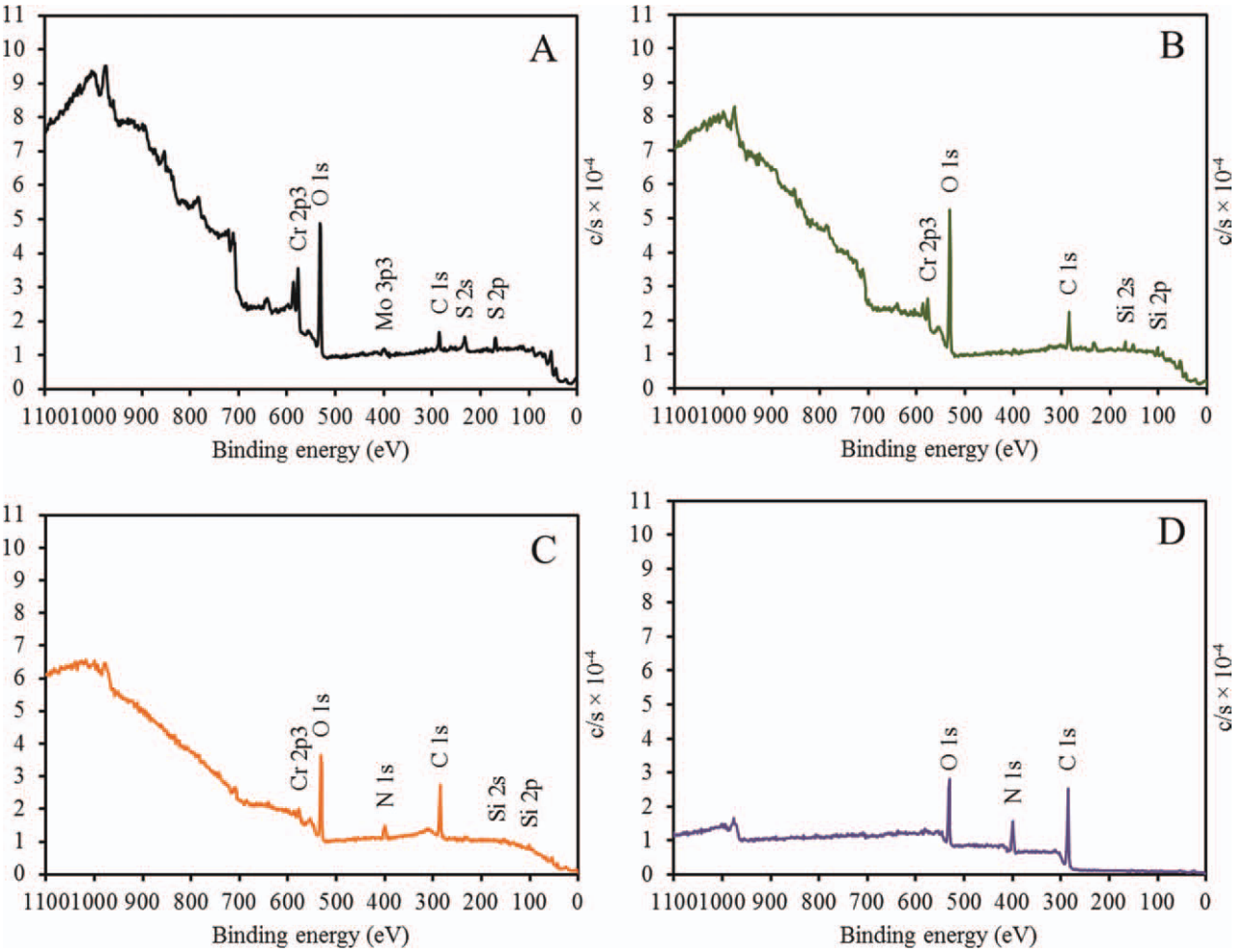

Figure 8. Representative survey XPS spectra of control (A), GOPTS modified (B), single multilayer modified (C), and characteristic spectrum from two to six multilayer modified stainless steel (D). [Color figure can be viewed in the online issue, which is available at wileyonlinelibrary.com.]

the high resolution spectrum of Si 2p showed two bands of which the highest values fell approximately at 102–101 and 104–103 eV, corresponding to the chemical species of Si—O—C and Si—O—Si, respectively [Figure 9(C)]. This demonstrates the formation of the covalent bond between the substrate (stainless steel) and GOPTS, as well as the formation of covalent bonds between molecules of GOPTS. After piranha solution treatment, —OH groups are formed, which are able to react with GOPTS forming covalent bonds after curing. Then, the covalently attached molecules of GOPTS are able to crosslink with themselves. The high resolution spectrum of C 1s from the treatments with 1–6 ML presented three bands from its deconvolution, and that can be attributed to the chemical species C—C/C—H, C—O, and N—C=O, in the ranges of 284–285 eV, 285–286 eV, and 287–288 eV, respectively [Figure 9(D)]. For the treatment with one multilayer, the band found in the 287–288 eV range may also include the C—O and C=O/O—C=O chemical species, that fell in the same range. Similar results have been observed in previous studies involving the interaction between PEI and substances containing carboxylic acids, as well as in studies involving GOPTS and its incorporation in oxidized surfaces.[26,35,36] This confirms the formation of amides from the reaction between the carboxylic acid groups of PAA and the primary amines of PEI. Overall, the XPS results support those of grazing angle FTIR. When interpreted in parallel with the ellipsometry data, the experimentally determined atomic percentages gained by XPS analysis closely match theoretical atomic percentages of the predicted surface chemistry, suggesting that the desired layer-by-layer N-halamine surface modifications were successfully achieved.

Antimicrobial Activity

The ability of the N-halamine modified stainless steel to inactivate viable microorganisms was demonstrated by incubation of control and modified stainless steel to an aqueous suspension of *Listeria monocytogenes*. After 6 h, bacterial suspensions incubated with unmodified stainless steel had approximately 10^4–10^5 CFUmL^{-1}, while N-halamine modified steel reduced the number of viable organisms by 1.51 ± 0.6 logarithmic cycles (i.e., a 99.7% reduction in viable organisms). These results demonstrate the potential for antimicrobial activity in our halamine modified steel.

Atomic Force Microscopy

Surface topography of control and modified stainless steel were characterized using AFM (Figure 10). Native, clean stainless

Table III. Representative Relative Percentages Obtained From the Deconvolution of High Resolution C 1s and Si 2p XPS Spectra

	C 1s					Si 2p	
Treatment	285–284 eV (C—C/C—H)	287–286 eV (C—O)	288–287 eV (C=O/O—C=O)	286–285 eV (C—N)	288–287 eV (N—C=O)	102–101 eV (Si—O—C)	104–103 eV (Si—O—Si)
Control	65.70	22.28	12.02				
GOPTS	51.66	37.96	10.38			91.57	8.43
One multilayer	50.62			33.56	15.82	79.02	20.98
Two multilayers	54.63			26.88	18.49		
Three multilayers	50.85			29.2	19.95		
Four multilayers	56.22			22.36	21.42		
Five multilayers	57.33			22.65	20.03		
Six multilayers	53.81			25.25	20.95		

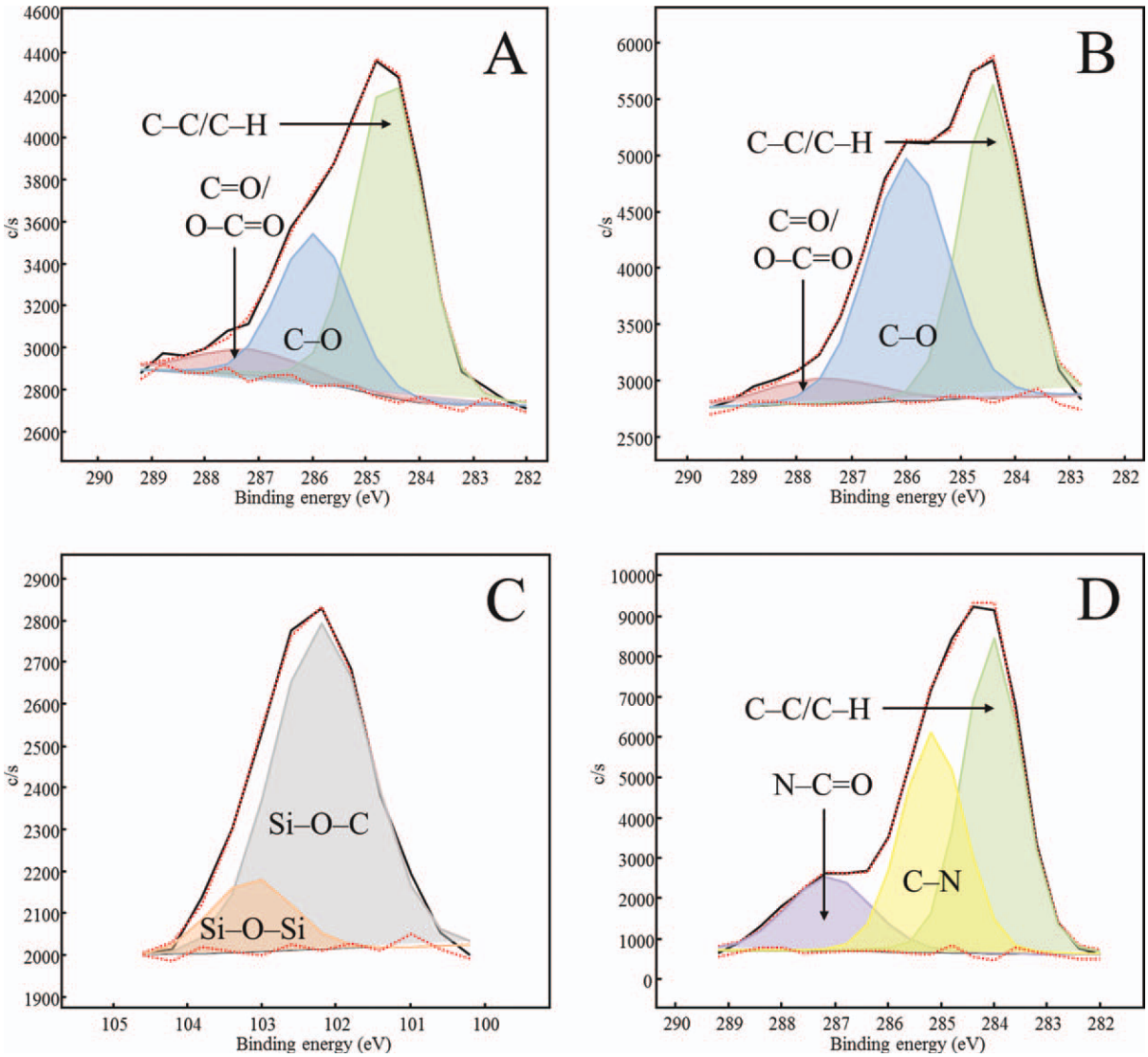

Figure 9. Representative deconvoluted high resolution XPS spectra. A and B represent the high resolution spectra of C 1s from Control and GOPTS modified steel, respectively; C represents the high resolution spectrum of Si 2p (GOPTS treatment); D shows a representative high resolution C 1s spectrum of stainless steel modified by deposition of one to six N-halamine forming multilayers. [Color figure can be viewed in the online issue, which is available at wileyonlinelibrary.com.]

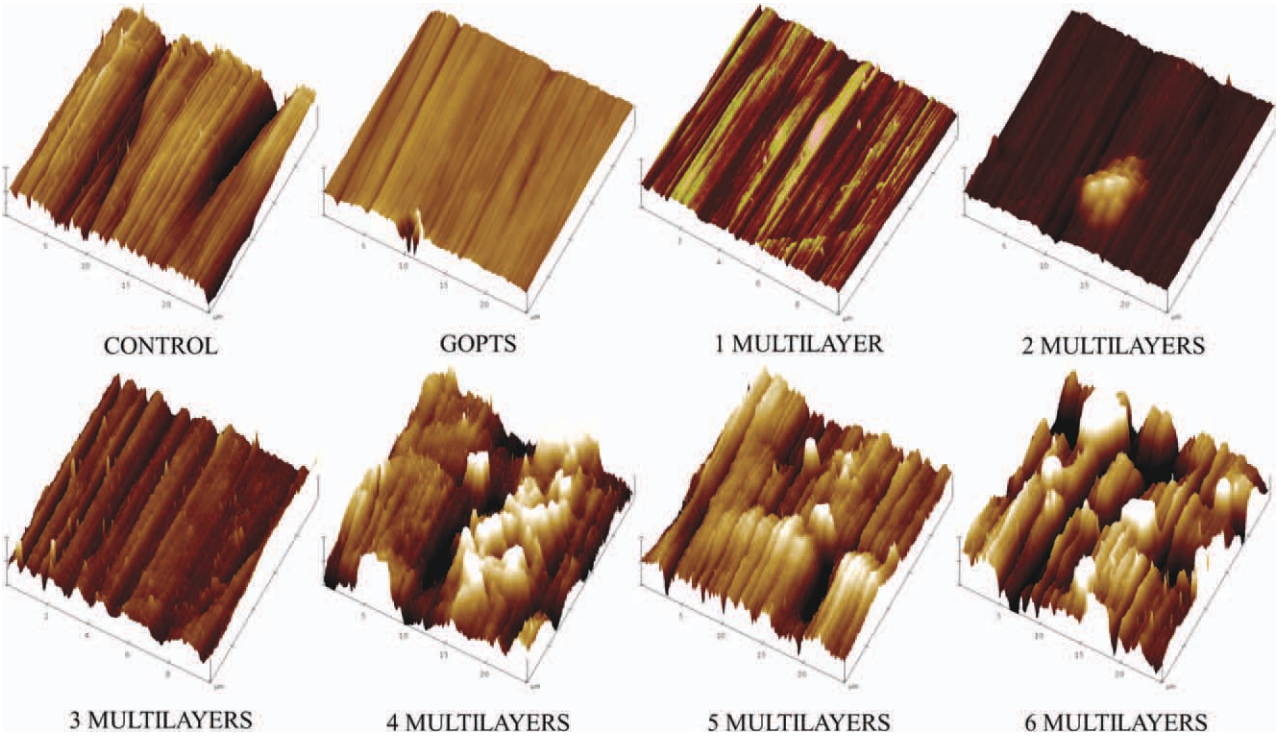

Figure 10. Representative atomic force micrographs for control and modified stainless steel. Vertical axis divisions represent 30 nm. [Color figure can be viewed in the online issue, which is available at wileyonlinelibrary.com.]

steel presents a surface roughness of 5.656 nm. A uniform, smooth, surface is observed after GOPTS treatment (2.656 nm roughness) up to the deposition of three multilayers (roughness values of 3.530 nm, 5.851 nm, and 3.738 nm for one, two, and three multilayers, respectively). The presence of surface irregularity after two multilayers may be the result of surface contamination or the beginning of the formation of "islands," as described above. Roughness values increase after four multilayers, presenting roughness values of 11.143 nm, 10.036 nm, and 13.384 nm for four, five, and six multilayers, respectively. The coalescence of discreet "islands" is more notable as the number of multilayers increases from four to six multilayers. These results support the conclusions drawn for ellipsometry results, suggesting the formation of isolated patches rather than a uniform surface coating. These results also suggest an increase in roughness with the deposition of additional multilayers, which may be a source of the variability observed in the contact angle analysis for the values of θ_A, θ_R, and H.

CONCLUSIONS

We have demonstrated the ability to modify the surface of 316 stainless steel using a covalent layer-by-layer deposition of N-halamine forming PEI and PAA. Prior work demonstrated that using similar chemistry, a single multilayer of PAA–PEI immobilized onto polyethylene film surfaces exhibited significant antimicrobial activity.[17] In addition to developing a surface modification technique to adapt such N-halamine modification to stainless steel, our goal in this work was to evaluate the influence of increasing multilayers on the number of available antimicrobial N-halamines. However, to retain bulk material properties, we wanted to limit the changes in surface chemistry to the top 100 nm or less. For this reason, we limited the number of multilayers evaluated in this study to six. Formation of covalent bonds was confirmed through FTIR and XPS between PEI and PAA, as well as the covalent attachment of GOPTS to the substrate's surface. Results of surface analysis in this work are in agreement with other reports in which PAA and PEI are immobilized onto supports in a layer-by-layer fashion.

Chlorination assays confirmed that the increasing quantity of amides and amines which present with increasing multilayer deposition were able to be chlorinated to form antimicrobial N-halamine moieties. The N-halamine-modified steel demonstrated antimicrobial activity (1.51 logarithmic reductions or 99.7% reduction in viable organisms) against *Listeria monocytogenes*, an important food-borne pathogen. On-going research is evaluating techniques to improve the uniformity of distribution across the stainless steel surface, and to quantify the effect of increasing N-halamine functionality on antimicrobial activity against pathogenic microorganisms.

ACKNOWLEDGMENTS

This material is based upon work supported by the National Institute of Food and Agriculture, US Department of Agriculture under project number 2011-65210-20059 and in part by the Center for Hierarchical Manufacturing at UMass Amherst, an NSF Nanoscale Science & Engineering Center supported by the

National Science Foundation under NSF Grant No. CMMI-0531171. The authors would also like to thank Prof. D. Julian McClements for use of his Kruss DCA for contact angle analysis, Prof. Lynne McLandsborough for assistance with antimicrobial activity assays, and Prof. Dr. Thomas J. McCarthy for use of his Rudolph SLII for ellipsometry measurements.

REFERENCES

1. Centers for Disease Control and Prevention, CDC. *MMWR: Morbidity and Mortality Weekly Report* **2004,** *53*, 338.
2. Centers for Disease Control and Prevention, CDC. *MMWR: Morbidity and Mortality Weekly Report* **2003,** *52*, 613.
3. Simões, M.; Simões, L. C.; Vieira, M. J. *LWT-Food Sci. Technol.* **2010,** *43*, 573.
4. Møretrø, T.; Langsrud, S. *J. Food Prot.* **2011,** *74*, 1200.
5. Maukonen, J.; Matto, J.; Wirtanen, G.; Raaska, L.; Mattila-Sandholm, T.; Saarela, M. *J. Ind. Microbiol. Biotechnol.* **2003,** *30*, 327.
6. Niinomi, M. *J. Artif. Org.* **2008,** *11*, 105.
7. Gupta, R.; Kumar, A. *Biomed. Mater.* **2008,** *3*, 034005.
8. Cloete, T.; Jacobs, L. *Water SA* **2001,** *27*, 21.
9. Kreske, A. C.; Ryu, J.; Pettigrew, C. A.; Beuchat, L. R. *J. Food Prot.* **2006,** *69*, 2621.
10. Marques, S. C.; Oliveira Silva Rezende, Jaine das Gracas; de Freitas Alves, L. A.; Silva, B. C.; Alves, E.; de Abreu, L. R.; Piccoli, R. H. *Braz. J. Microbiol.* **2007,** *38*, 538.
11. Oulahal, N.; Brice, W.; Martial, A.; Degraeve, P. *Food Control* **2008,** *19*, 178.
12. Parkar, S.; Flint, S.; Brooks, J. *J. Appl. Microbiol.* **2004,** *96*, 110.
13. Sharma, M.; Ryu, J.; Beuchat, L. *J. Appl. Microbiol.* **2005,** *99*, 449.
14. Eknoian, M.; Worley, S.; Harris, J. *J. Bioact. Compat. Polym.* **1998,** *13*, 136.
15. Worley, S.; Sun, G. *Trend Polym. Sci.* **1996,** *4*, 364.
16. Sun, Y.; Sun, G. *J. Appl. Polym. Sci.* **2002,** *84*, 1592.
17. Goddard, J. M.; Hotchkiss, J. H. *J. Food Prot.* **2008,** *71*, 2042.
18. Kocer, H. B.; Akdag, A.; Worley, S. D.; Acevedo, O.; Broughton, R. M.; Wu, Y. *ACS Appl. Mater. Interf.* **2010,** *2*, 2456.
19. Liang, J.; Wu, R.; Wang, J.; Barnes, K.; Worley, S. D.; Cho, U.; Lee, J.; Broughton, R. M.; Huang, T. *J. Ind. Microbiol. Biotechnol.* **2007,** *34*, 157.
20. Anonymous, Code of federal regulations. Available at: http://www.access.gpo.gov/nara/cfr/waisidx_05/21cfrv3_05.html, Accessed December 20, **2011.**
21. American Society for Testing and Materials, ASTM D 2022–89. Standard Test Methods of Sampling and Chemical Analysis of Chlorine-Containing Bleaches, **2008.**
22. Uchida, E.; Uyama, Y.; Ikada, Y. *Langmuir* **1993,** *9*, 1121.
23. Mead, P.; Slutsker, L.; Dietz, V.; McCaig, L.; Bresee, J.; Shapiro, C.; Griffin, P.; Tauxe, R. *Emerg. Infect. Dis.* **1999,** *5*, 607.
24. Long, J.; Chen, P. *Adv. Colloid. Interface Sci.* **2006,** *127*, 55.
25. Adamson AW, G. A. Physical Chemistry of Surfaces; John Wiley & Sons Inc.: New York, NY, **1997.**
26. Makamba, H.; Hsieh, Y.; Sung, W.; Chen, S. *Anal. Chem.* **2005,** *77*, 3971.
27. Drelich, J.; Chibowski, E.; Meng, D. D.; Terpilowski, K. *Soft Mater.* **2011,** *7*, 9804.
28. Smith, B. C. Infrared Spectral Interpretation: A Systematic Approach; CRC Press: Boca Raton, FL, **1999.**
29. Plagge, A.; Adler, H.; Jaehne, E.; Paliwoda, G.; Rohwerder, M.; Stratmann, M.; Eichhorn, K. *Macromol. Mater. Eng.* **2007,** *292*, 1245.
30. Guzman, E.; Cavallo, J. A.; Chulia-Jordan, R.; Gomez, C.; Strumia, M. C.; Ortega, F.; Rubio, R. G. *Langmuir* **2011,** *27*, 6836.
31. Zhao, X.; Pan, F.; Lu, J. R. *Prog. Nat. Sci.* **2005,** *15*, 56.
32. Guzman, E.; Chulia-Jordan, R.; Ortega, F.; Rubio, R. G. *Phys. Chem. Chem. Phys.* **2011,** *13*, 18200.
33. Tsukruk, V.; Bliznyuk, V.; Visser, D.; Campbell, A.; Bunning, T.; Adams, W. *Macromolecules* **1997,** *30*, 6615.
34. Kim, Y. S.; Davis, R.; Cain, A. A.; Grunlan, J. C. *Polymer* **2011,** *52*, 2847.
35. Ma, P. C.; Kim, J.; Tang, B. Z. *Carbon* **2006,** *44*, 3232.
36. Pollock, N.; Fowler, G.; Twyman, L. J.; McArthur, S. L. *Chem. Commun.* **2007, 2482.**